The Journal of Experimental Biology 215, 2445-2454

doi:10.1242/jeb.058008

RESEARCH ARTICLE

Early developmental gene regulation in *Strongylocentrotus purpuratus* embryos in response to elevated CO_2 seawater conditions

LaTisha M. Hammond* and Gretchen E. Hofmann

Department of Ecology, Evolution and Marine Biology, University of California, Santa Barbara, CA 93106-9620, USA

*Author for correspondence at present address: Department of Biology, Georgetown University, Washington, DC 20057-1229, USA (lmh75@georgetown.edu)

SUMMARY

Ocean acidification, or the increased uptake of CO_2 by the ocean due to elevated atmospheric CO_2 concentrations, may variably impact marine early life history stages, as they may be especially susceptible to changes in ocean chemistry. Investigating the regulatory mechanisms of early development in an environmental context, or ecological development, will contribute to increased understanding of potential organismal responses to such rapid, large-scale environmental changes. We examined transcript-level responses to elevated seawater CO_2 during gastrulation and the initiation of spiculogenesis, two crucial developmental processes in the purple sea urchin, *Strongylocentrotus purpuratus*. Embryos were reared at the current, accepted oceanic CO_2 concentration of 380 microatmospheres (μatm), and at the elevated levels of 1000 and 1350 μatm, simulating predictions for oceans and upwelling regions, respectively. The seven genes of interest comprised a subset of pathways in the primary mesenchyme cell gene regulatory network (PMC GRN) shown to be necessary for the regulation and execution of gastrulation and spiculogenesis. Of the seven genes, qPCR analysis indicated that elevated CO_2 concentrations only had a significant but subtle effect on two genes, one important for early embryo patterning, *Wnt8*, and the other an integral component in spiculogenesis and biomineralization, *SM30b*. Protein levels of another spicule matrix component, SM50, demonstrated significant variable responses to elevated CO_2. These data link the regulation of crucial early developmental processes with the environment that these embryos would be developing within, situating the study of organismal responses to ocean acidification in a developmental context.

Key words: *Strongylocentrotus purpuratus*, development, gene regulatory network, molecular physiology, ocean acidification.

Received 20 March 2011; Accepted 14 March 2012

INTRODUCTION

Ecological development, or 'eco-devo', is the study of development in an ecological context, moving the study of development out of the laboratory and into the 'real world' environment (Gilbert, 2001; Sultan, 2007). Additionally, the aims of eco-devo are to incorporate 'both abiotic and biotic factors into studies of gene expression and regulatory pathways … [and study] the expression of traits important to function, fitness and ecological interactions in [the] environment' (Sultan, 2007). Understanding how regulatory pathways operate under differential environmental conditions has been suggested as the necessary next step for developmental and physiological studies, as environmental factors play a crucial role in the execution of development (Gilbert, 2005; Sultan, 2007; Gilbert and Epel, 2009).

The need for an ecological perspective on development has become increasingly clear in light of anthropogenically driven ocean warming and ocean acidification (Kurihara, 2008; Doney et al., 2009; Dupont et al., 2010). Very little is known about the capacity for phenotypic plasticity in organisms during their early life history stages and whether they can successfully respond to rapidly changing environmental conditions. The anthropogenically driven rise in atmospheric CO_2, which has steadily increased since the industrial revolution, has led to an increase in oceanic CO_2 (Forster et al., 2007; IPCC, 2007; Feely et al., 2008) and to ocean acidification (Doney et al., 2009; Feely et al., 2009). The continued rise in oceanic CO_2 could present challenges for many marine organisms, as the increasingly acidic water is potentially corrosive to those organisms with calcified hard parts (Feely et al., 2008) and can interfere with the extracellular and intracellular acid–base balance necessary for proper cellular functions (Fabry, 2008).

Given that early developmental processes are especially sensitive to environmental perturbation (Hamdoun and Epel, 2007; Epel, 2003), successful development relies heavily on physiological tolerance of the environment and on whether embryos and larvae are able to respond to changing abiotic factors. There are a growing number of studies that have investigated how marine invertebrate embryos and larvae may handle changes in carbonate chemistry as a consequence of ocean acidification (Kurihara, 2008; Dupont and Thorndyke, 2009; Byrne, 2011). Many of these studies have focused on mortality and phenotypic characteristics such as growth rate and structural and morphological changes in larvae (see Kurihara, 2008). Specifically, the calcium carbonate spicules and skeletons of larval echinoids are directly affected by changes in oceanic CO_2 concentration (Kurihara and Shirayama, 2004; Kurihara, 2008; Dupont et al., 2008; Byrne et al., 2009; O'Donnell et al., 2010). Few studies, however, have investigated the molecular-level responses and signaling pathways that regulate phenotypic expression and responses relative to large-scale environmental changes like ocean acidification (see Sultan, 2007; Todgham and Hofmann, 2009; O'Donnell et al., 2010). In this study, we sought to make the connection between these larger scale environmental phenomena and molecular-level responses. We measured expression changes in two regulatory pathways in a key gene regulatory network

– the primary mesenchyme cell gene regulatory network (PMC GRN) – in *Strongylocentrotus purpuratus* sea urchin embryos as they develop through gastrulation at elevated CO_2 levels. Notably, we chose CO_2 levels that are consistent with future emission scenarios predicted by the IPCC (Meehl et al., 2007) and, additionally, reflect occasional high P_{CO_2} exposures for *S. purpuratus* embryos in episodic upwelling zones on the coast of the northeastern Pacific (Feely et al., 2009; Hauri et al., 2009).

Of the numerous processes in early development, gastrulation is an extremely critical one that, if not executed properly, has dire and typically fatal results for the embryo (Wolpert, 1992; Leptin, 2005). In sea urchin embryos, the gastrulation process overlaps another key process, spiculogenesis. A group of spiculogenesis-specific cells, the primary mesenchyme cells (PMCs), ingress and migrate during gastrulation, and initiate the events leading to the formation of the spicules (Wilt, 2005). Not surprisingly, many of the regulatory pathways that regulate the initiation of spiculogenesis are also crucial for the regulation of cellular movements in gastrulation (Oliveri et al., 2008; Ettensohn, 2009). These shared pathways make up part of the PMC GRN, which regulates the process of biomineralization (the process by which organisms take up minerals in order to form their hard parts). The PMC GRN is one of the best understood gene regulatory networks in sea urchins (Oliveri et al., 2008; Ettensohn, 2009), providing a detailed model of the cascade of gene regulatory events required of the embryo to carry out gastrulation and spiculogenesis. While many studies have utilized the PMC GRN as a model to garner an increased fundamental and mechanistic understanding of these two crucial aspects of the urchin developmental program, no studies to date have sought to determine whether and how environmental factors, such as increased CO_2, can affect the transcriptional regulation of these processes by the PMC GRN.

In this study, we investigated how a subset of regulatory pathways for two developmental processes in *S. purpuratus* embryos were affected by elevated CO_2 concentrations in comparison with embryos that develop under control conditions. Aside from being a model organism with a thoroughly characterized PMC GRN, *S. purpuratus* was chosen as the study organism because it is a keystone echinoderm species that inhabits a large biogeographic range along the North American west coast. Additionally, *S. purpuratus* larvae, like other echinoplutei, develop a calcium carbonate ($CaCO_3$) skeleton that is susceptible to increases in oceanic CO_2 (Kurihara and Shirayama, 2004; O'Donnell et al., 2009; Dupont et al., 2010). We have investigated a subset of key pathways, which either regulate or are regulated by the gene *Alx1*, in the PMC GRN that are crucial for the developmental processes of gastrulation and spiculogenesis.

An overview of the targeted PMC GRN genes

Alx1 is an upstream PMC GRN regulatory gene that is essential for PMC ingression and their movement within the blastocoel (Ettensohn et al., 2007). The genes chosen for this study were in pathways that either regulate or are regulated by *Alx1*. These genes (shown in Fig. 1) were *Wnt8*, *Pmar1*, *Alx1*, *VegFR*, *SM30b*, *Msp130* and *SM50*. *Alx1* itself is regulated by *Pmar1*, a zygotically expressed transcriptional repressor responsible for activating micromere specification (micromeres that are then specified to become the PMCs) (Oliveri et al., 2008). *Wnt8* is a zygotically expressed regulatory gene that regulates *Pmar1* through the activation of β-catenin (Oliveri et al., 2008). As one of the earliest genes to activate the PMC GRN, *Wnt8* is associated with cell fate determination through canonical signaling pathways and is important for the morphogenetic movement of the PMCs through non-canonical signaling (Leptin, 2005).

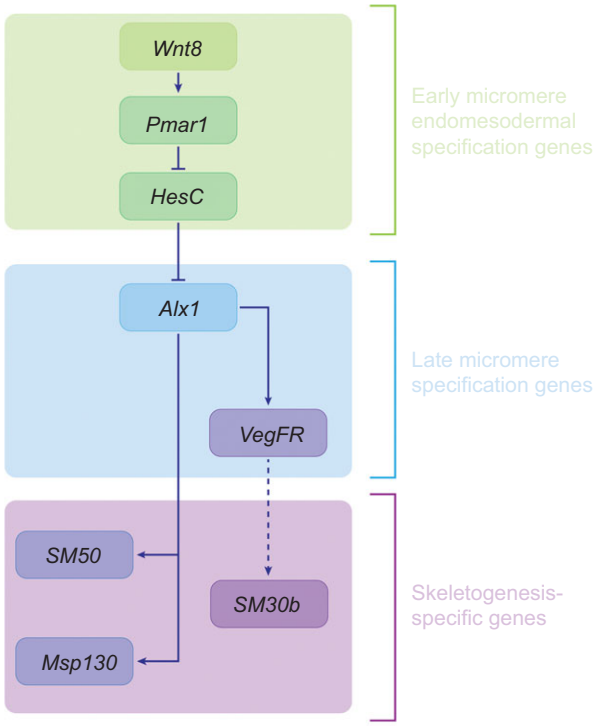

Fig. 1. Simplified diagram of the seven targeted genes of interest and their specific pathways highlighted within the primary mesenchyme cell gene regulatory network (PMC GRN). Arrows indicate direct regulatory input and bars represent repression of expression. Dashed line indicates non-confirmed direct interaction (modified from Oliveri et al., 2008). *Wnt8*, one of the earliest genes to activate the PMC GRN, is associated with cell fate determination through canonical signaling pathways, and is important for the morphogenetic movement of the PMCs through non-canonical signaling (Leptin, 2005). *Pmar1* (paired-class micromere anti-repressor 1) has been proposed to be part of a 'double-repressor gate' because it prevents the expression of *HesC*, which encodes a repressor that prevents the specification of skeletogenic fate in all the cells in the embryos except the micromeres (Revilla-i-Domingo et al., 2007; Oliveri and Davidson, 2007) (reviewed in Oliveri et al., 2008; Ettensohn, 2009). *Alx1* (aristaless-like homeobox 1) is essential for activating functional pathways and multiple gene batteries in the downstream PMC GRN; specifically, the biomineralization genes. *VegFR* (vascular endothelial growth factor receptor), which is expressed solely by the PMCs, encodes a receptor of the ectoderm-derived ligand VegF (vascular endothelial growth factor) (Ettensohn, 2009) and the signaling between VegF and VegFR is necessary for the correct migration and orientation of the PMCs, and proper spicule formation (Duloquin et al., 2007). Additionally, VegF/VegFR signaling is thought to be the regulatory input to one of the terminal differentiation genes of the PMC GRN, *SM30b*. *SM30b* (spicule matrix 30b) is a biomineralization gene that encodes the spicule matrix protein SM30, which is important for spicule rod growth and elongation (Kitajima and Urakami, 2000; Urry et al., 2000). *Msp130* encodes a PMC-specific cell-surface glycoprotein (Illies et al., 2002) and it has been suggested to play a role in Ca^{2+} sequestration and/or deposition during spicule formation. *SM50* (spicule matrix 50) is a gene that encodes spicule matrix protein SM50, which is important for spicule elongation (Kitajima and Urakami, 2000; Urry et al., 2000), and is necessary for deposition of the calcite spicule rudiment (Wilt et al., 2008b).

Alx1 also acts as a regulatory input to *VegFR*. *VegFR*, which is expressed solely by the PMCs, encodes a receptor of the ectoderm-derived ligand VegF (vascular endothelial growth factor) (Ettensohn, 2009). VegF originates from the two ventrolateral positions in the ectoderm where the triradiate spicule rudiments are later deposited

(Okazaki and Inoue, 1976), and this ectoderm–PMC interaction between VegF and VegFR is necessary for the correct migration and orientation of the PMCs, and proper spicule formation (Duloquin et al., 2007). Additionally, VegF/VegFR signaling is thought to be the regulatory input to one of the terminal differentiation genes of the PMC GRN, *SM30b* (Duloquin et al., 2007; Oliveri et al., 2008). *SM30b* is a biomineralization gene important for spicule rod growth and elongation (Kitajima and Urakami, 2000; Urry et al., 2000). It encodes the spicule matrix protein SM30, one of over four dozen identified spicule matrix proteins that make up the occluded matrix of the spicule (Wilt, 2005; Livingston et al., 2006).

Msp130, also regulated by *Alx1*, is a terminal differentiation gene that encodes a cell surface glycoprotein, MSP130, which completely surrounds the PMCs and the spicules (Kiyomoto et al., 2007; Wilt et al., 2008a). *Msp130* has been implicated in calcium deposition (Carson et al., 1985). Lastly, *Alx1* acts as a regulatory input for *SM50*, a gene that encodes another spicule matrix protein, SM50. SM50, like SM30, occurs within the occluded matrix of the spicule (Wilt, 2005; Livingston et al., 2006); it is important for spicule elongation (Kitajima and Urakami, 2000; Urry et al., 2000) and is necessary for deposition of the calcite spicule rudiment (Wilt et al., 2008a).

We have evaluated the expression of this subset of PMC GRN genes in response to varying levels of CO_2 during early development; specifically, over the course of gastrulation. We also investigated whether expression of a protein encoded by one of the biomineralization genes (*SM50*) varied as a result of differential CO_2 levels. Investigating these pathways will not only provide information on how upstream PMC GRN events affect biomineralization and spicule formation but also help us to elucidate how the developmental programs of spiculogenesis and gastrulation respond to increased CO_2 and ocean acidification.

MATERIALS AND METHODS

Strongylocentrotus purpuratus collection and embryo culturing

Adult *S. purpuratus* (Stimpson 1857) were collected in the Santa Barbara Channel during the middle of the spawning season (mid-February 2010) and held in flow-through seawater tanks at 14–16°C. Individuals were spawned by coelomic injection of 0.5 mol l^{-1} KCl within 2–3 weeks of collection. Eggs from a single female were then fertilized by a single male, following a protocol outlined elsewhere (Foltz et al., 2004), in ambient CO_2 seawater to ensure the highest fertilization success as low pH levels can compromise this process (Havenhand et al., 2008; Parker et al., 2009) (but see Byrne et al., 2009; Byrne et al., 2010). Only batches of eggs with a fertilization success of >90% were used. A total of four mating pairs were spawned and eggs fertilized.

Embryos from each mating pair were divided approximately equally and raised in larval culture buckets in the CO_2 delivery system (see Fangue et al., 2010) at a density of ~100 embryos ml^{-1}. Because of the physical constraints of the CO_2 delivery system, only 12 culture buckets could be run at a time. To maximize the number of mating pairs and replicates within the 12 bucket system, embryos from two mating pairs were raised simultaneously in two sets of six larval culture buckets. Of the six larval buckets used for each mating pair, two buckets had a CO_2 concentration of 380 microatmospheres (μatm), which served as the controls, two treatment buckets had a CO_2 concentration of ~1000 μatm, and the remaining two treatment buckets had a concentration of ~1350 μatm Therefore, each treatment had two replicates per mating pair (totaling six culture buckets). Each set of 12 buckets was referred to as a 'trial' for statistical analyses. Four mating pairs were used; therefore two trials were run (i.e. a total of 24 buckets run at 12 buckets at a time). The temperature of all larval culture buckets was maintained at ~15°C.

Seawater chemistry

During the embryo culturing described above, seawater chemistry was performed using a Mettler-Toledo T50 (Columbus, OH, USA) alkalinity titrator and a spectrophotometric pH assay as described previously (Fangue et al., 2010). In preparation for the experiments, pH and alkalinity measurements were taken every few hours until the seawater reached the desired CO_2 concentration, and once the desired conditions were achieved (see Table 1 for summary data for seawater chemistry), spawning was performed and embryos were introduced into the culture buckets. During embryo culturing, pH was measured at all embryo sampling time points while alkalinity was measured once during the 19 h sampling period. Following the protocol outline by Fangue (Fangue et al., 2010) (see also DOE, 1994), in brief, the seawater from each culture was filtered of embryos and siphoned into separate, pre-warmed (25°C) sampling cuvettes. The increase from 15 to 25°C was corrected for later using a carbonate calculator (Lewis and Wallace, 1998) described below. Each cuvette was filled and capped with no head space to minimize CO_2 exchange with the atmosphere. Each sample was measured before and after addition of the indicator dye *m*-Cresol Purple. The absorbance wavelengths measured corresponded to one non-absorbing and two absorption maxima for the *m*-Cresol Purple indicator. Final pH values were determined using the absorbance values and the pH determination calculations in the modified standard operating procedures (see DOE, 1994). The accuracy of these results was ensured by periodic measurement of a certified reference material (CRM) for pH (Ocean Carbon Dioxide Quality Control, Scripps Institute of Oceanography) (Fangue et al., 2010). Total alkalinity measurements were made as previously described (Fangue et al., 2010). Briefly, seawater was siphoned and filtered, ensuring no air bubbles or embryos, into 125 ml borosilicate glass-stoppered bottles (1500-125, Corning, Corning, NY, USA) bottles, allowed to overflow, capped and brought to 25°C for immediate measurement *via* titration. The total alkalinity (μmol kg^{-1}), along with the corresponding pH measurement, were then entered into the CO2SYS carbonate calculator (Lewis and Wallace, 1998) with the pre-determined dissociation constant for carbonic acid (Mehrbach et al., 1973) to determine the concentrations of dissolved inorganic carbon (DIC) and P_{CO_2}, the remaining parameters needed to fully characterize the carbonate system in seawater and fully characterize the amount of CO_2 in the seawater sample (Fangue et al., 2010).

Table 1. Summary of total alkalinity (TA), CO_2 and pH values

CO_2 treatment (μatm)	TA (μmol kg^{-1})	Actual CO_2 concentration (μatm)	pH
380	2218±8.7	389±23	8.055±0.022
1000	2219±4.2	973±25	7.699±0.008
1350	2218±5.7	1364±20	7.621±0.004

Actual CO_2 concentrations were calculated using CO2SYS calculator (Lewis and Wallace, 1998) with the pre-determined dissociation constant for carbonic acid (Mehrbach et al., 1973).

Table 2. PMC GRN gene-specific primer sequences used for qPCR

Gene	Forward primer (5′→3′)	Reverse primer (5′→3′)
Wnt8	ACAACGAGGCTGGCAGAAA	AGACGCCATGACACTTACAGGTT
Pmar1	ATCCACCATCCTCGCATTCA	TTCCGCTTACGACCGATGA
Alx1	CAGCGACGACGTCAAGTCA	TCTTGGCATCGCTGTCGTT
Msp130	CCGAGGTCCAGCGATTGA	CACCCAACTGACCTGTGTAAGG
SM30b	GTTCTCCGGTAGGCAAACA	ACATTTTGGGGCAAATGAAA
SM50	AGAACCCCATGTCAGGACCACC	AAACGAAAGCGCGCATGG
VegFR	AGGGCAGGTCAACAGTTCAG	GGCAACCAATTTGACATCCT
ef1-α	CAAAGAAATCGTCAGGGAGGTC	AGATTGGGATGAAGGGCACAG

PMC, primary mesenchyme cell; GRN, gene regulatory network.

Embryo sampling

Embryo samples were collected by reverse filtration at three time points during the experiment: (1) directly after hatching and PMC ingression (21 h post-fertilization, h.p.f.), (2) at primary invagination (30 h.p.f.) and (3) at full gastrula (36 h.p.f.). Each of the samples (which contained ~40,000 whole embryos per sample) were homogenized by vortexing in 500 µl of TRIzol Reagent (Invitrogen, Carlsbad, CA, USA) and stored at –80°C until RNA extraction. Total RNA was extracted using the TRIzol manufacturer's protocol with the following modifications. Once homogenized, samples were thawed, passed through a 25 gauge needle 3–5 times and washed with 100 µl chloroform, and the RNA was precipitated with 125 µl isopropanol + 125 µl precipitation salt solution (1.2 mol l^{-1} NaCl, 0.8 mol l^{-1} disodium citrate in DEPC-treated RNase-free water). The RNA was re-suspended in nuclease-free water and RNA concentrations were measured and purity was checked using a Nanodrop ND-1000 full-spectrum UV/Vis spectrophotometer (NanoDrop Technologies, Wilmington, DE, USA).

Gene expression analysis using qPCR

Following extraction, 100 ng total RNA was reverse transcribed to synthesize cDNA using oligo dT and the ImProm-II Reverse Transcription System (Promega, Madison, WI, USA) following the manufacturer's protocol. The resulting cDNA was amplified *via* quantitative real-time PCR (qPCR) using primers for the PMC GRN-specific genes: *Wnt8*, *Pmar1*, *Alx1*, *Msp130*, *SM30b*, *SM50* and *VegFR* (Table 2). Gene-specific primers for *Wnt8*, *Pmar1*, *Alx1*, *Msp130*, *SM30b*, *SM50* and *ef1-α* were designed using Primer Express software (version 2.0.0; Applied Biosystems, Foster City, CA, USA) with the published *S. purpuratus* sequences for *ef1-α* (GenBank accession no. NM_001123497.1), *Wnt8* (SPU_020371), *Pmar1* (SPU_01422), *Alx1* (SPU_214644), *Msp130* (SPU_013821), *SM30b* (SPU_000826) and *SM50* (SPU_018811). Confirmed primer sequences for *VegFR* were obtained from SpBase (http://www.spbase.org/SpBase/resources/methods/q-pcr.php).

Briefly, qPCR was carried out in 20 µl SYBR Green Supermix (Bio-Rad, Hercules, CA, USA) reactions containing 2 µl of template cDNA and 1 µl of each primer. The qPCR reactions were run with the following protocol: 1 cycle at 95°C for 3 min, 40 cycles at 58°C for 10 s and 95°C for 1 min, 1 cycle at 55°C for 1 min. Melt curve analyses were also conducted to ensure only a single product for each primer set was amplified. Relative mRNA levels were quantified as follows. *Wnt8*, *Pmar1*, *Alx1*, *Msp130*, *SM30b*, *SM50*, *VegFR* and *ef1-α* cycle threshold (Ct) values were first normalized to a single *S. purpuratus* embryo standard control sample run on every qPCR plate. Four, 10-fold serial dilutions of this standard were used to develop a standard curve on each plate and Ct results from all samples were expressed relative to these curves. The Ct values were then normalized to the corresponding *ef1-α* values. The *ef1-α* gene was used as an internal control as its expression does not significantly differ in response to elevated CO_2. The resulting normalized values are the reported relative concentrations for *Wnt8*, *Pmar1*, *Alx1*, *Msp130*, *SM30b*, *SM50* and *VegFR*.

Quantification of spicule matrix protein SM50

To determine whether elevated CO_2 differentially affected the translation of transcripts for the terminal differentiation genes, protein analysis was carried out on *SM50*. Approximately 1500 embryos were collected from each culture at each sampling time point for protein extraction and immunoblot analysis of SM50 protein. Embryos were collected by microcentrifugation, all seawater was removed, and the samples were immediately snap-frozen and stored at –80°C.

Whole-embryo samples were homogenized by sonication in a lysis buffer containing 1.4× protease inhibitor cocktail (Roche, Pleasanton, CA, USA), 1 µg ml^{-1} leupeptin, 0.1% NP-40 substitute, 100 mmol l^{-1} DTT and 100 mmol l^{-1} PMSF. Samples were quantified using the BCA assay (Pierce Biotechnologies, Rockford, IL, USA), and 10 µg of homogenate from each sample was dissolved in sample loading dye and heated at 100°C for 3 min. Proteins were resolved on a 4% stacking/12% resolving discontinuous SDS-page gel and electrophoretically transferred to Hybond ECL 0.45 µm nitrocellulose membrane (GE Healthcare, Piscataway, NJ, USA). Blots were washed with phosphate-buffered saline (PBS) and blocked overnight in 5% non-fat dry milk in PBS with 0.1% Tween-20 at 4°C. Blots were then incubated in primary antibody (polyclonal antisera prepared in rabbits against SM50 at a 1:500 dilution in blocking buffer, courtesy of Dr Fred Wilt) (Killian and Wilt, 1996) for 1 h at room temperature, washed in PBS with 0.1% Tween-20, and then incubated in secondary antibody [goat anti-rabbit horseradish peroxidase conjugate (BioRad) at 1:5000 dilution in blocking buffer] for 1.5 h at room temperature. Blots were developed in chemiluminescent SuperSignal West Dura Extended Duration Substrate (Pierce Biotechnologies) and imaged using Quantity One software and VersaDoc imaging system (BioRad). Blots were quantified and analyzed with ImageJ (http://lukemiller.org/index.php/2010/11/analyzing-gels-and-western-blots-with-image-j/). Sample intensities were quantified relative to intensities of a standard protein extract (*S. purpuratus* prism stage embryos); 10 µg of standard were loaded onto each gel to ensure relative intensities of SM50 on each gel could be directly compared.

Statistical analyses

Statistical analyses were performed using JMP 8.0 (SAS). For each gene, MANOVA analyses were conducted to determine the significance of CO_2 on the expression of each gene, with CO_2, trial and mating pair nested within trial as factors. A MANOVA was also used to test for differences in SM50 protein levels with CO_2,

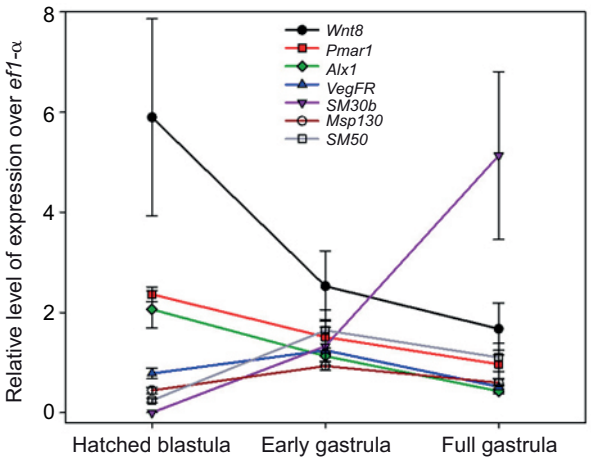

Fig. 2. Summary of gene expression in all seven genes of interest at the control CO_2 concentration of 380 µatm at hatched blastula, early gastrula and full gastrula developmental stages. All N=4 (representing mate pairs) except *Pmar1* where N=3. Error bars indicate s.e.m. For definitions of gene names, see Fig. 1.

trial and mating pair nested within trial as factors. Stages were analyzed separately using one-way ANOVA and *post hoc* Tukey–Kramer HSD was used to determine differences between CO_2 concentrations.

RESULTS

Overview of expression profiles at control CO_2 concentrations

For control conditions, embryos were raised under 380 µatm CO_2, an accepted level of ambient CO_2 that yields a control pH of ~8.1, and transcript levels for the seven candidate genes were evaluated using qPCR at three time points between hatched blastula and gastrula stages (Fig. 2). All transcripts were present at detectable levels at all three time points and generally matched patterns of expression observed in other studies (see below for details of individual genes). Of the genes evaluated in this study, *Wnt8* exhibited the highest level of expression between hatched blastula and gastrula stage, consistent with the requirement for *Wnt8* signaling in multiple regulatory pathways in the embryo (e.g. endoderm specification and non-skeletogenic mesoderm specification as well as PMC specification) (Smith and Davidson, 2008).

At hatched blastula stage, *Wnt8* exhibited the highest level of expression. Expression of *Pmar1* and *Alx1* were the next highest, and were similar in expression levels to each other. *VegFR* and *Msp130* exhibited a lower level of expression, followed by *SM50* and *SM30b*, exhibiting the lowest transcript levels (Fig. 2). At early gastrula stage, *Wnt8* expression decreased significantly, but was still greater than that of all other genes. *Pmar1* and *Alx1* transcript levels also decreased and were similar to those of *VegFR* and *Msp130*. *VegFR*, *Msp130*, *SM50* and *SM30b* displayed increases in transcript level. At full gastrula stage, *Wnt8* transcript levels further decreased but, again, were still higher than those of the other genes. Expression of *Pmar1* and *Alx1* also exhibited a further decrease in expression. *VegFR*, *Msp130* and *SM50* all displayed decreases and had similar transcript levels. In contrast, *SM30b* transcript levels increased significantly by this developmental stage, an expression pattern consistent with previous findings (Guss and Ettensohn, 1997; Wei et al., 2006).

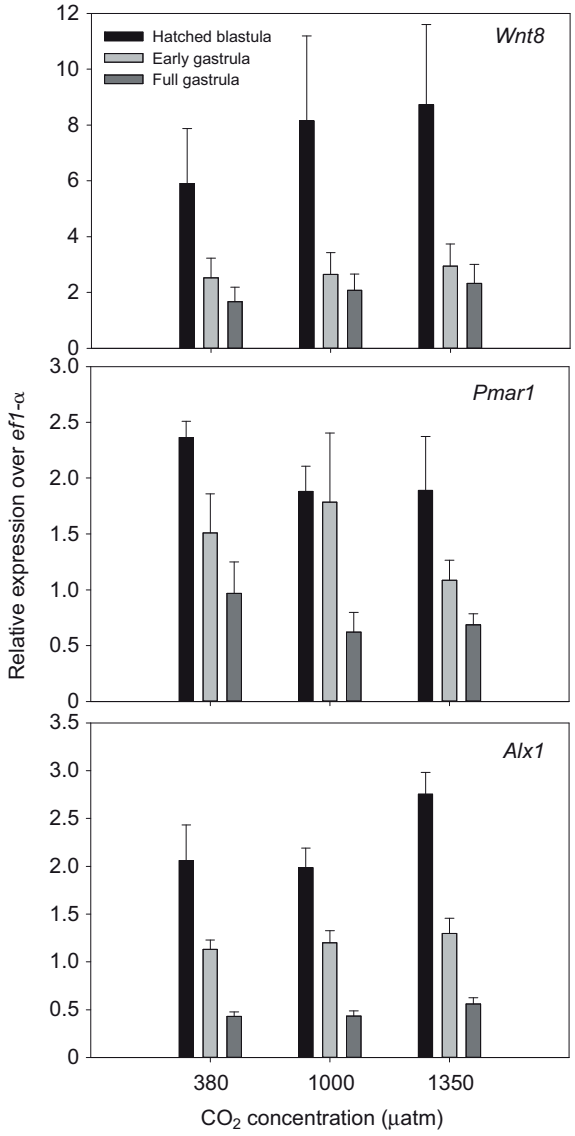

Fig. 3. Expression of the upstream genes *Wnt8*, *Pmar1* and *Alx1* at hatched blastula, early gastrula and full gastrula stages at CO_2 concentrations of 380, 1000 and 1350 µatm. All N=4 (representing mating pairs) except *Pmar1* where N=3. Error bars indicate s.e.m. For definitions of gene names, see Fig. 1.

Patterns of gene expression in embryos developing under high CO_2 conditions

Wnt8

As a general pattern, *Wnt8* expression declined as development advanced. At the control CO_2 concentration of 380 µatm, the expression profile was as follows: *Wnt8* expression was highest at hatched blastula stage, decreased at early gastrula (P=0.0449) and further decreased at gastrula (P<0.0080; Fig. 3). Expression profiles were similar at 1000 and 1350 µatm CO_2. MANOVA results indicate that *Wnt8* expression varied significantly as a function of CO_2 concentration across development (P=0.0042). Expression also varied with trial (P<0.0001). There was also a significant interaction between CO_2 and trial (P=0.0136); however, this effect simply highlights the variation between mating pairs, as mating pair was nested within trial. A separate ANOVA and *post hoc* analysis

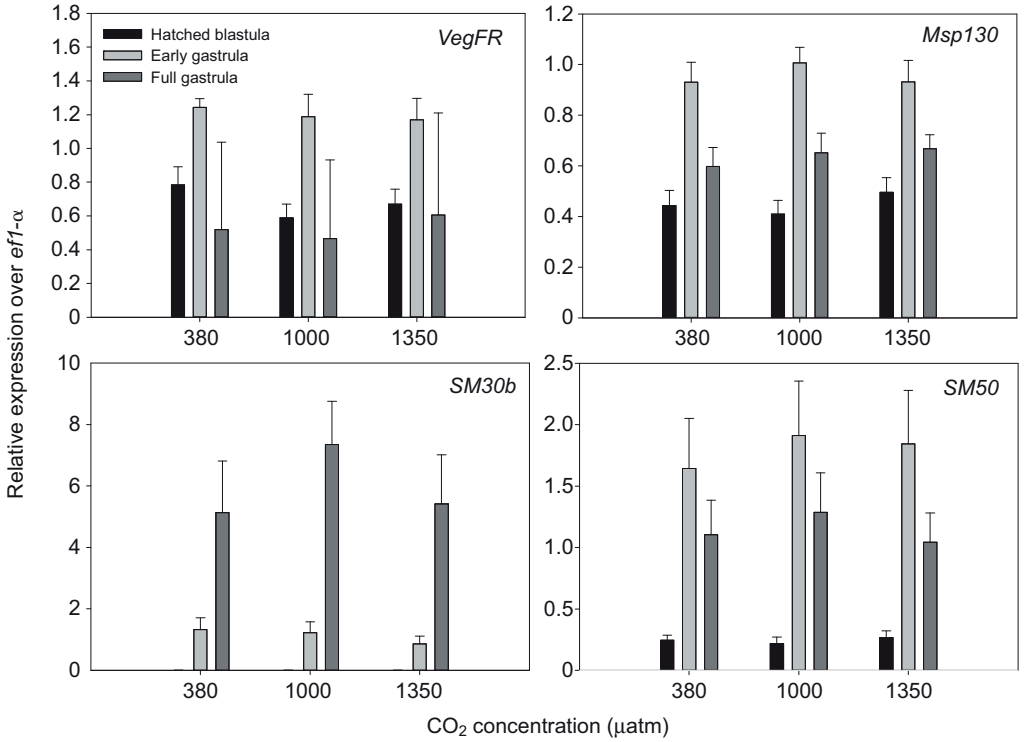

Fig. 4. Expression of the downstream genes *VegFR*, *Msp130*, *SM30b* and *SM50* at hatched blastula, early gastrula and full gastrula stages at CO_2 concentrations of 380, 1000 and 1350 μatm. All N=4 (representing mating pairs). Error bars indicate s.e.m. For definitions of gene names, see Fig. 1.

revealed that there was a significant increase in expression from 380 to 1350 μatm at full gastrula stage (P=0.0217).

Pmar1

Under control conditions of 380 μatm, *Pmar1* expression was highest at hatched blastula stage, decreased slightly at early gastrula and further decreased at full gastrula. When embryos developed under high CO_2, there were different outcomes for the two CO_2 treatments: the pattern of expression was similar to that of the control for the 1350 μatm CO_2 treatment, whereas at 1000 μatm there was some variation (Fig. 3). Specifically, there was a decrease in hatched blastula expression, an increase at early gastrula stage and a decrease at full gastrula stage. However, these shifts in expression observed in the mid-CO_2 level treatment were not significant (all P>0.05; Fig. 3). Thus, expression of *Pmar1* during early development was not affected by elevated CO_2 concentrations (MANOVA, P=0.2342). There was also no variation due to trial, nor was there a significant interaction between CO_2 and trial (P=0.2867). Furthermore, for embryos at all three CO_2 concentrations, expression at full gastrula stage was significantly lower than at hatched blastula stage (P=0.0012).

Alx1

At the control CO_2 concentration of 380 μatm, transcript for *Alx1* showed an overall reduction as development proceeded: *Alx1* gene expression was highest at the hatched blastula stage, decreased at the early gastrula stage, and further decreased at the full gastrula stage. The expression profiles at 1000 and 1350 μatm were nearly identical to the expression profile at 380 μatm (Fig. 3). There was no significant variation in *Alx1* expression as a result of CO_2 (MANOVA, P=0.2126), but there was a significant effect of trial (MANOVA, P<0.0001). For all CO_2 concentrations, expression at hatched blastula stage was significantly greater than that of early gastrulae (P=0.0016) and full gastrulae (P<0.0001). At hatched blastula stage, *Alx1* expression was highest at 1350 μatm; however, this was non-significant (P=0.0700).

VegFR

Under control CO_2 conditions, *VegFR* transcript levels were highest at early gastrula stage and lowest at full gastrula stage. The general expression pattern was the same at 1000 and 1350 μatm (Fig. 4). Overall, there was no effect of CO_2 concentration on *VegFR* expression (MANOVA, P=0.2562), nor was there any variation attributable to trial (MANOVA, P=0.5245) or a significant interaction between CO_2 concentration and trial (MANOVA, P=0.4192). At each CO_2 concentration, expression at hatched blastula stage was significantly lower than that at early gastrula (P=0.0014) and significantly higher than that at full gastrula (P=0.0089).

SM30b

At 380 μatm CO_2, *SM30b* transcript levels were very low at hatched blastula stage, increased significantly at early gastrula, and further increased at full gastrula stage, where expression was greatest. The same trend was true for embryos cultured at 1000 and 1350 μatm CO_2 (Fig. 4). *SM30b* expression, however, did vary as a function of CO_2 concentration through development (MANOVA, P=0.0163), as indicated by increased expression at 1000 μatm in full gastrula stage. There was also variation as a result of trial (MANOVA, P=0.0181). The effects of CO_2 concentration and trial were independent of each other (MANOVA, P=0.5557). At each CO_2 concentration, the increase in expression from hatched blastula stage to early gastrula (P<0.0001) and full gastrula stage (P<0.0001) was highly significant.

Msp130

At the control CO_2 concentration of 380 μatm, *Msp130* expression was highest at early gastrula stage and lowest at hatched blastula

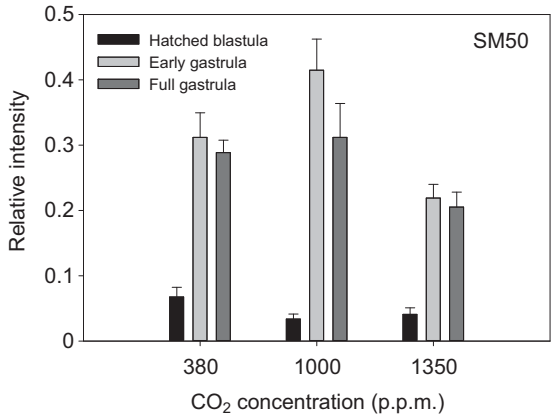

Fig. 5. SM50 protein expression at hatched blastula, early gastrula and full gastrula stages at CO_2 concentrations of 380, 1000 and 1350 µatm. *N*=4 (representing mating pairs). Error bars indicate s.e.m.

stage at each CO_2 concentration (Fig. 4). *Msp130* expression did not vary as a result of CO_2 concentration (MANOVA, P=0.3419). However, expression did vary as a result of trial (MANOVA, P=0.0004), which was independent of CO_2 (MANOVA, P=0.4040). The expression at early gastrula stage was significantly higher than hatched blastula expression (P<0.0001), and the increase in expression at full gastrula over hatched blastula stage was also significant (P=0.0117).

SM50 gene expression and protein levels

Under control conditions, *SM50* transcript levels were lowest at hatched blastula stage, increased at early gastrula, where expression was highest, and decreased at full gastrula stage at 380, 1000 and 1350 µatm CO_2 (Fig. 4). Expression throughout development did not vary as a function of CO_2 concentration (MANOVA, P=0.7506) but did vary with trial (MANOVA, P=0.0012). There was no interaction between CO_2 concentration and trial (MANOVA, P=0.9127). At all CO_2 concentrations, *SM50* gene expression at hatched blastula stage was significantly lower than at early gastrula stage (P<0.0001) and full gastrula stage (P<0.0001).

Conversely, while there was no significant effect of CO_2 on *SM50* transcript levels, there was a significant effect on SM50 protein levels (MANOVA, P<0.0001; Fig. 5). SM50 protein level from embryos at each CO_2 concentration followed the same expression pattern as *SM50* transcript level: expression was lowest at hatched blastula stage, increased at early gastrula, where expression was greatest (P<0.0001 relative to hatched blastula), and decreased slightly at full gastrula stage but was still significantly greater than expression at hatched blastula (P<0.0001). SM50 protein expression did vary within trials (MANOVA, P<0.0001). There was also a significant interaction between CO_2 and trial (MANOVA, P=0.0119). However, the interaction was caused by expression in embryos at 1000 µatm displaying a slightly different expression pattern from that in embryos at 380 and 1350 µatm – early gastrula stage embryos at 1000 µatm displayed greater expression than embryos at both 380 and 1350 µatm. One-way ANOVA (with Bonferroni-corrected α=0.0167) results at each stage show that embryos at hatched blastula stage at 1000 µatm (P=0.0006) and 1350 µatm (P=0.0044) displayed significantly lower SM50 protein levels than those at 380 µatm. At early gastrula stage, embryos at 1000 µatm exhibited the greatest expression level, which was significantly greater than that at 1350 µatm (P=0.0002) but not that at 380 µatm (P=0.1867). Protein expression at 380 µatm was greater than that at 1350 µatm, but this was not significant (P=0.0493). Finally, there were no significant differences between CO_2 treatments at full gastrula stage (P=0.0261).

DISCUSSION

The molecular exploration of embryonic gene regulatory networks is extensive, but placing the study of regulatory pathways within these networks in an ecological or environmental context is relatively unexplored. In this study, a subset of key pathways in the PMC GRN necessary for gastrulation and the initiation of spiculogenesis (see Fig. 1) were investigated in embryos reared at relevant, elevated CO_2 levels through gastrulation. With regard to the effects of ocean acidification conditions on development, the results of this study revealed only subtle changes in *SM30b* and *Wnt8* expression at the high CO_2 concentrations of 1000 and 1350 µatm, and variable expression in a biomineralization-specific protein, SM50. Additionally, *Alx1*, *Pmar1*, *VegFR*, *Msp130* and *SM50* were unaffected in terms of transcript level and timing of expression (for a summary, see Table 3).

Embryo and micromere specification genes

The CO_2 concentration of 1350 µatm had a significant effect on *Wnt8* expression at full gastrula stage: transcript levels were 20–28% greater than control levels at this stage. An increase in *Wnt8* transcript level of this magnitude may not adversely affect the embryo, as no morphological abnormalities were observed in these embryos (not shown). Significant overexpression would likely have caused abnormalities such as the multiple invagination sites around the embryo found in a previous study (Wikramanayake et al., 2004). Given the current data and lack of morphological abnormalities, it may be that 1350 µatm, while causing some change in *Wnt8*

Table 3. Summary of expression changes in embryos at hatched blastula, early gastrula and full gastrula stages at elevated CO_2 concentrations

	1000 µatm			1350 µatm		
Gene	Hatched blastula	Early gastrula	Full gastrula	Hatched blastula	Early gastrula	Full gastrula
Wnt8	–	–	–	–	–	↑
Pmar1	–	–	–	–	–	–
Alx1	–	–	–	–	–	–
VegFR	–	–	–	–	–	–
SM30b	–	–	↑	–	–	–
Msp130	–	–	–	–	–	–
SM50	–	–	–	–	–	–

Data indicate the response to CO_2 treatment relative to control (380 µatm CO_2).
– indicates no significant change; arrows denote direction of change in gene expression.

Table 4. Summary of the role each targeted gene plays during early development, the change in gene expression and the possible implications for *S. purpuratus* embryos

Gene	Role/function//gene information	Response to elevated CO_2		Predictions/implications of response to elevated CO_2
		1000 μatm	1350 μatm	
Wnt8	Endomesodermal specification, embryo patterning, early PMC-GRN regulator	–	↑ at full gastrula stage	Gastrulation (*via* endomesodermal specification and embryo patterning) may be compensated for at high CO_2
Pmar1	Upstream repressor of PMC specification and skeletogenic micromere lineage repressor	–	–	Repressor expression and function presumably not affected
Alx1	Activator of skeletogenic micromere lineage	–	–	No significant effect on activation and regulation of skeletogenic micromere lineage
VegFR	Ectoderm ligand receptor; regulatory input into *SM30b*; involved in proper migration and orientation of the PMCs	–	–	No significant effect on PMC migration and orientation
SM30b	Biomineralization; regulates spicule growth	↑ at full gastrula stage	–	Upregulation may reflect ability to compensate for elevated CO_2; regulation of spicule rudiment and early spicule formation may be uninterrupted
Msp130	Biomineralization; hypothesized role in Ca^{2+} sequestration	–	–	Ca^{2+} sequestration for spicule formation may not be interrupted
SM50	Biomineralization; spicule rudiment deposition and elongation	–	–	Transcription regulating spicule rudiment deposition and elongation unaffected

– indicates no significant change; arrows denote direction of change in gene expression.

expression at full gastrula stage, may not interfere with the initiation and regulation of embryo patterning, endoderm specification and, by extension, gastrulation.

Another study (Todgham and Hofmann, 2009) that explored the transcriptomic response to ocean acidification in *S. purpuratus* at prism stage (~40 h.p.f.) found that *Wnt8* expression was decreased at the 540 μatm CO_2 level and exhibited no change at ~1020 μatm. Differences in embryo responses between that study and the current study at the CO_2 concentration of ~1000 μatm are likely a result of the use of a microarray approach by Todgham and Hofmann, compared with the present qPCR-based study. Additionally, differences may be attributed to developmental stage, as in the latter, early prism stage *Wnt8* expression levels are already significantly lower than those of earlier stages under normal conditions (Wikramanayake et al., 2004).

The present data indicate that elevated CO_2 did not alter *Alx1* expression. *Alx1* is necessary for specification and morphogenetic movement of the PMCs, while also activating the genes necessary for the epithelial mesenchymal transitions of gastrulation (Ettensohn et al., 2003; Wu and McClay, 2007). *Alx1* expression was also found to activate expression of downstream genes in the PMC GRN that are in turn essential for activation of biomineralization genes (such as *Msp130* and *SM50*) (Ettensohn et al., 2003). Therefore, the current data suggest that PMC ingression and the subsequent initiation of the morphogenetic movements of gastrulation would be unaffected by elevated CO_2. Morphological studies of early developmental stages exposed to elevated CO_2 (Hammond, 2010) indeed show this; gastrulation proceeds successfully although with a possible modest delay in timing. Given that *Pmar1* expression also did not change in response to elevated CO_2 levels, a change in *Alx1* expression would not be anticipated. It is important to note, however, that recent data suggest that *Alx1* expression is not solely regulated by *Pmar1*. Sharma and Ettensohn, using pharmacological inhibitors of MEK and WMISH with *LvEts1*, demonstrated that while *Alx1* is activated by *Pmar1*, its expression is maintained by MAPK signaling and expression of *ets1*, another transcriptional regulator in the PMC GRN (Sharma and Ettensohn, 2010); thus, *ets1* expression under elevated CO_2 conditions should also be considered. The present data contrast with those of Todgham and Hofmann, who observed a decrease in *Alx1* expression at 1020 μatm in prism (~40 h.p.f.) stage *S. purpuratus* (Todgham and Hofmann, 2009). As noted above, these differences may be due to the different developmental stages evaluated and different quantification methods used in each of the studies.

Skeletogenesis-specific genes and proteins

The *SM30b* expression pattern observed here is similar to previous findings (e.g. Oliveri et al., 2008; Killian et al., 2010) where expression in the PMCs begins at ingression and continues steadily after this (Guss and Ettensohn, 1997; Livingston et al., 2006). Previous work (Duloquin et al., 2007) has demonstrated that, unlike the other terminal biomineralization genes in the PMC GRN that are regulated predominately by the *Alx1* signaling cascade, *SM30* expression is largely activated by the ectodermal signaling of VegF/VegFR. As CO_2 did not perturb *VegFR* expression, the CO_2 induced changes in *SM30b* expression at full gastrula stage must have occurred by an undetermined mechanism independent of *VegFR*. Moreover, because spiculogenesis and spicule rudiment formation have been shown to occur normally in embryos raised at 1000 μatm (Hammond, 2010), such an increase in *SM30b* expression at 1000 μatm suggests that at this CO_2 concentration the embryo may upregulate *SM30b* as a way of compensating for the heightened CO_2 conditions and to ensure spiculogenesis continues. In contrast, O'Donnell and colleagues observed downregulation of *SM30-like* expression in early *Lytechinus pictus* echinoplutei in response to a CO_2 concentration of 970 μatm (O'Donnell et al., 2010). However, these findings were in a much later developmental stage, possibly explaining the differences in expression in response to CO_2 (i.e. expression at the initiation of spiculogenesis *vs* expression after significant completion of the larval skeleton). Additionally, variation in response could be related to species-specific differences. Further studies should elucidate the variable patterns of expression in *S. purpuratus*.

The pattern of expression of *Msp130* exhibited in this study is similar to previous findings (Guss and Ettensohn, 1997) with a peak in *Msp130* expression at early gastrula stage. *Msp130* encodes a PMC-specific cell-surface glycoprotein (Illies et al., 2002). While the exact function of *Msp130* is unclear, it has been suggested to

play a role in Ca^{2+} sequestration and/or deposition during spicule formation as the *N*-linked oligosaccharide chain on the Msp130 protein binds Ca^{2+} (Carson et al., 1985; Farach-Carson et al., 1989). As elevated CO_2 did not affect the expression of *Msp130*, if Msp130 protein is indeed necessary for Ca^{2+} sequestration and deposition, then CO_2 levels up 1350 µatm may not interfere with Ca^{2+} uptake and transport.

SM50 gene expression and and protein levels

SM50 gene expression typically begins between hatched blastula stage and PMC ingression (Guss and Ettensohn, 1997) and follows the pattern observed in the current study. *SM50* gene expression is necessary for spicule elongation. Blockage of the gene and protein by injection of morpholino antisense oligonucleotides has been shown to prevent biomineralization (Peled-Kamar et al., 2002; Wilt et al., 2008b). Elevated CO_2 concentrations up to 1350 µatm appeared to have no effect on *SM50* expression (Fig. 4). Given that one of the confirmed regulatory inputs into *SM50*, *Alx1* (Oliveri et al., 2008), was not affected by 1350 µatm CO_2, the lack of a shift in *SM50* transcript levels is not surprising. As *SM50* appears to be necessary for the deposition of the spicule rudiment (Wilt et al., 2008b), uninterrupted *SM50* expression would ensure minimal interference with calcite crystal deposition in high CO_2 seawater, a notion which is supported by findings that elevated CO_2 up to 1000 µatm did not negatively affect the timing of spicule deposition in *S. purpuratus* gastrulae (Hammond, 2010). It is important to note that there is evidence that the deposition of the calcite crystal and spicule elongation are two different processes; the deposited rudiment is pure calcite crystal whereas spicule elongation involves the conversion of deposited amorphous calcium carbonate to calcite over time in the elongating spicule (Beniash et al., 1997; Ingersoll and Wilt, 1998; Peled-Kamar et al., 2002; Wilt et al., 2008b).

The difference in expression between *SM50* transcript levels and SM50 protein levels suggests that elevated CO_2 could have an effect on translation rates or protein stability. The significant increase in levels of SM50 protein in early gastrula stage embryos at 1000 µatm *vs* control CO_2 levels suggests that the embryos respond to CO_2 at a post-transcriptional level, though whether this is specific to SM50 alone or is a general effect on the proteome is not known. Interestingly, however, the significant decrease in SM50 protein levels at high CO_2 levels (1350 µatm) suggests that the embryo may not able to compensate for such a high CO_2 concentration. Such a depression may result in negative interference with spicule deposition or elongation; however, further studies into spiculogenesis at elevated CO_2 are needed to determine whether CO_2 concentrations at this level have an effect on spicule deposition or elongation.

CONCLUSION

The results of this study demonstrate that many of the genes in a subset of PMC GRN genes were unaffected by elevated levels of CO_2, and for those that were, the increases, while significant, were only subtle at different life history stages (see summary in Table 4). Interestingly, one of these genes with slightly increased expression was *Wnt8*, which may reflect the ability of the embryo to compensate for increased CO_2 by upregulating this gene, which is necessary for the initiation of the PMC GRN. The slightly increased expression of *Wnt8* has positive implications for the process of gastrulation; embryo patterning and endomesodermal specification are most likely unaffected. The second of the affected genes was the biomineralization-specific *SM30b*. Upregulation of this gene suggests the continued ability to initiate and carry out spiculogenesis. Furthermore, while expression of another biomineralization gene, *SM50*, did not vary with elevated CO_2, the protein it encodes, SM50, displayed an increase in expression at 1000 µatm, but a decrease in expression at 1350 µatm, suggesting the embryo may initially be able to compensate for the increased CO_2 by increasing the translation or stability of SM50, but as CO_2 increases, this ability may be compromised, with potential negative effects on spicule deposition and elongation.

While further studies are needed to clarify the variable responses to elevated CO_2, including studies comparing transcription and translation, it appears that early developmental and skeletogenic gene expression in *S. purpuratus* embryos was little affected, suggesting that these embryos may be somewhat resilient at the molecular level with regard to elevated CO_2 concentrations. Given recent work suggesting that coastal organisms in the eastern Pacific may be exposed to acidic, high P_{CO_2} seawater as a result of seasonal, episodic upwelling more regularly than once believed (Feely et al., 2009; Hauri et al., 2009), the seeming robustness is not altogether surprising. The seasonal, potentially long-term exposures experienced by *S. purpuratus*, a keystone benthic species along the North American west coast, may have allowed for some degree of adaptation to elevated CO_2 concentrations.

The present study is one of the first to investigate embryonic responses to elevated CO_2 in PMC GRN-specific genes, especially those upstream of the terminal biomineralization genes. Moreover, it attempts to connect the expression of genes involved in crucial developmental processes and gene batteries to the changing environmental conditions caused by anthropogenically driven CO_2-induced ocean acidification. The ecological development approach to understanding the possible consequences for early life history stages will increase our understanding of key developmental processes in context while enabling a greater ability to forecast how marine organisms will or will not respond to their rapidly changing environments.

ACKNOWLEDGEMENTS

We would like to thank Dr Andrew Dickson (Scripps Institution of Oceanography) for his support in developing protocols for our 'in-house' seawater analysis, Anna MacPherson for assistance with sample collection and water chemistry, and Dr Pauline Yu for guidance with protein analysis. Additionally, we would like to thank Dr Steven Gaines for statistical advice and Dr Kathleen Foltz for insightful comments.

FUNDING

This study was supported in part by a National Science Foundation (NSF) GRFP Fellowship to L.M.H., an NSF grant [OCE 0425107] to G.E.H., and funds from the University of California in support of a multi-campus research program, *Ocean Acidification: A Training and Research Consortium* (http://oceanacidification.msi.ucsb.edu/) to G.E.H.

REFERENCES

Beniash, E., Aizenberg, J., Addadi, L. and Weiner, S. (1997). Amorphous calcium carbonate transforms into calcite during sea urchin larval spicule growth. *Proc. R. Soc. Lond. B* **264**, 461-465.

Byrne, M. (2011). Impact of ocean warming and ocean acidification on marine invertebrate life history stages: vulnerabilities and potential for persistence in a changing ocean. In *Oceanography and Marine Biology: An Annual Review*, Vol. 49 (ed. R. N Gibson, R. J. A. Atkinson and J. D. M. Gordon), pp. 1-42. Boca Raton, FL: CRC Press.

Byrne, M., Ho, M., Selvakumaraswamy, P., Nguyen, H. D., Dworjanyn, S. A. and Davis, A. R. (2009). Temperature, but not pH, compromises sea urchin fertilization and early development under near-future climate change scenarios. *Proc. Biol. Sci.* **276**, 1883-1888.

Byrne, M., Soars, N. A., Ho, M. A., Wong, E., McElroy, D., Selvakumaraswamy, P., Dworjanyn, S. A. and Davis, A. R. (2010). Fertilization in a suite of coastal marine invertebrates from se Australia is robust to near-future ocean warming and acidification. *Mar. Biol.* **157**, 2061-2069.

Carson, D. D., Farach, M. C., Earles, D. S., Decker, G. L. and Lennarz, W. J. (1985). A monoclonal antibody inhibits calcium accumulation and skeleton formation in cultured embryonic cells of the sea urchin. *Cell* **41**, 639-648.

DOE (1994). *Handbook of Methods for the Analysis of the Various Parameters of the Carbon Dioxide System in Sea Water*, version 2 (ed. A. G. Dickson and C. Goyet), ORNL/CDIA-74. Oak Ridge, TN: US Department of Energy.
Doney, S. C., Fabry, V. J., Feely, R. A. and Kleypas, J. A. (2009). Ocean acidification: the other CO_2 problem. *Annu. Rev. Mar. Sci.* **1**, 169-192.
Duloquin, L., Lhomond, G. and Gache, C. (2007). Localized VEGF signaling from ectoderm to mesenchyme cells controls morphogenesis of the sea urchin embryo skeleton. *Development* **134**, 2293-2302.
Dupont, S. and Thorndyke, M. C. (2009). Impact of CO_2-driven ocean acidification on invertebrates early life-history – what we know, what we need to know and what we can do. *Biogeosciences Discuss.* **6**, 3109-3131.
Dupont, S., Havenhand J., Thorndyke, W., Peck, L. and Thorndyke, M. (2008). Near-future level of CO_2-driven ocean acidification radically affects larval survival and development in the brittlestar *Ophiothrix fragilis*. *Mar. Ecol. Prog. Ser.* **373,** 285-294.
Dupont, S., Ortega-Martínez, O. and Thorndyke, M. (2010). Impact of near-future ocean acidification on echinoderms. *Ecotoxicology* **19**, 449-462.
Epel, D. (2003). Protection of DNA during early development: adaptations and evolutionary consequences. *Evol. Dev.* **5**, 83-88.
Ettensohn, C. A. (2009). Lessons from a gene regulatory network: echinoderm skeletogenesis provides insights into evolution, plasticity and morphogenesis. *Development* **136**, 11-21.
Ettensohn, C. A., Illies, M. R., Oliveri, P. and De Jong, D. L. (2003). Alx1, a member of the Cart1/Alx3/Alx4 subfamily of paired-class homeodomain proteins, is an essential component of the gene network controlling skeletogenic fate specification in the sea urchin embryo. *Development* **130**, 2917-2928.
Ettensohn, C. A., Kitazawa, C., Cheers, M. S., Leonard, J. D. and Sharma, T. (2007). Gene regulatory networks and developmental plasticity in the early sea urchin embryo: alternative deployment of the skeletogenic gene regulatory network. *Development* **134**, 3077-3087.
Fabry, V. J. (2008). Ocean science. Marine calcifiers in a high-CO_2 ocean. *Science* **320**, 1020-1022.
Fangue, N. A., O'Donnell, M. J., Sewell, M. A., Matson, P. G., MacPherson, A. C. and Hofmann, G. E. (2010). A laboratory-based, experimental system for the study of ocean acidification effects on marine invertebrate larvae. *Limnol. Oceanogr. Methods* **8**, 441-452.
Farach-Carson, M. C., Carson, D. D., Collier, J. L., Lennarz, W. J., Park, H. R. and Wright, G. C. (1989). A calcium-binding, asparagine-linked oligosaccharide is involved in skeleton formation in the sea urchin embryo. *J. Cell Biol.* **109**, 1289-1299.
Feely, R. A., Sabine, C. L., Hernandez-Ayon, J. M., Ianson, D. and Hales, B. (2008). Evidence for upwelling of corrosive 'acidified' water onto the continental shelf. *Science* **320**, 1490-1492.
Feely, R. A., Doney, S. C. and Cooley, S. R. (2009). Ocean acidification: present conditions and future changes in a high-CO_2 world. *Oceanography* **22**, 36-47.
Foltz, K. R., Adams, N. L. and Runft, L. L. (2004). Echinoderm eggs and embryos: procurement and culture. *Methods Cell Biol.* **74**, 39-74.
Forster, P., Ramaswamy, V., Artaxo, P., Berntsen, T., Betts, R., Fahey, D. W., Haywood, J., Lean, J., Lowe, D. C., Myhre, G. et al. (2007). Changes in atmospheric constituents and in radiative forcing. In *Climate Change 2007: The Physical Science Basis. Contribution of Working Group I to the Fourth Assessment Report of the Intergovernmental Panel on Climate Change* (ed. S. Solomon, D. Qin, M. Manning, Z. Chen, M. Marquis, K. B. Averyt, M. Tignor and H. L. Miller), pp. 129-234. Cambridge: Cambridge University Press.
Gilbert, S. F. (2001). Ecological developmental biology: developmental biology meets the real world. *Dev. Biol.* **233**, 1-12.
Gilbert, S. F. (2005). Mechanisms for the environmental regulation of gene expression: ecological aspects of animal development. *J. Biosci.* **30**, 65-74.
Gilbert , S. F. and Epel, D. (2009). *Ecological Development Biology: Integrating Epigenetics, Medicine, and Evolution*. Sunderland, MA: Sinauer Associates.
Guss, K. A. and Ettensohn, C. A. (1997). Skeletal morphogenesis in the sea urchin embryo: regulation of primary mesenchyme gene expression and skeletal rod growth by ectoderm-derived cues. *Development* **124**, 1899-1908.
Hamdoun, A. and Epel, D. (2007). Embryo stability and vulnerability in an always changing world. *Proc. Natl. Acad. Sci. USA* **104**, 1745-1750.
Hammond, L. M. (2010). Physiological response to environmental variation in strongylocentrotus purpuratus early developmental stages. PhD dissertation, University of California, Santa Barbara.
Hauri, C., Gruber, N., Plattner, G. K., Alin, S., Feely, R. A., Hales, B. and Wheeler, P. A. (2009). Ocean acidification in the California current system. *Oceanography* **22**, 60-71.
Havenhand, J. N., Buttler, F. R., Thorndyke, M. C. and Williamson, J. E. (2008). Near-future levels of ocean acidification reduce fertilization success in a sea urchin. *Curr. Biol.* **18**, R651-R652.
Illies, M. R., Peeler, M. T., Dechtiaruk, A. M. and Ettensohn, C. A. (2002). Identification and developmental expression of new biomineralization proteins in the sea urchin *Strongylocentrotus purpuratus*. *Dev. Genes Evol.* **212**, 419-431.
Ingersoll, E. P. and Wilt, F. H. (1998). Matrix metalloproteinase inhibitors disrupt spicule formation by primary mesenchyme cells in the sea urchin embryo. *Dev. Biol.* **196,** 95-106.
IPCC (2007). *Climate Change 2007: Synthesis Report Contributions of Working Groups I, II and III to the Fourth Assessment Report of the Intergovernmental Panel on Climate Change* (ed. Core Writing Team, R. K. Pachuri and A. Reisinger). Geneva: IPCC.
Killian, C. E. and Wilt, F. H. (1996). Characterization of the proteins comprising the integral matrix of *Strongylocentrotus purpuratus* embryonic spicules. *J. Biol. Chem.* **271**, 9150-9159.
Killian, C. E., Croker, L. and Wilt, F. H. (2010). SpSM30 gene family expression patterns in embryonic and adult biomineralized tissues of the sea urchin, strongylocentrotus purpuratus. *Gene Expr. Patterns* **10**, 135-139.
Kitajima, T. and Urakami, H. (2000). Differential distribution of spicule matrix proteins in the sea urchin embryo skeleton. *Dev. Growth Differ.* **42**, 295-306.
Kiyomoto, M., Zito, F., Costa, C., Poma, V., Sciarrino, S. and Matranga, V. (2007). Skeletogenesis by transfated secondary mesenchyme cells is dependent on extracellular matrix-ectoderm interactions in *Paracentrotus lividus* sea urchin embryos. *Dev. Growth Differ.* **49**, 731-741.
Kurihara, H. (2008). Effects of CO_2-driven ocean acidification on the early developmental stages of invertebrates. *Mar. Ecol. Prog. Ser.* **373**, 275-284.
Kurihara, H. and Shirayama, Y. (2004). Effects of increased atmospheric CO_2 on sea urchin early development. *Mar. Ecol. Prog. Ser.* **274**, 161-169.
Leptin, M. (2005). Gastrulation movements: the logic and the nuts and bolts. *Dev. Cell* **8**, 305-320.
Lewis, E. and Wallace, D. W. R. (1998). Program developed for CO_2 system calculations. ORNL/CDIAC-105. Oak Ridge, TN: US Department of Energy.
Livingston, B. T., Killian, C. E., Wilt, F., Cameron, A., Landrum, M. J., Ermolaeva, O., Sapojnikov, V., Maglott, D. R., Buchanan, A. M. and Ettensohn, C. A. (2006). A genome-wide analysis of biomineralization-related proteins in the sea urchin *Strongylocentrotus purpuratus*. *Dev. Biol.* **300**, 335-348.
Meehl, G. A., Stocker, T. F., Collins, W. D., Friedlingstein, P., Gaye, A. T., Gregory, J. M., Kitoh, A., Knutti, R., Murphy, J. M., Noda, A. et al. (2007). Global climate projections. In *Climate Change 2007: The Physical Science Basis. Contribution of Working Group I to the Fourth Assessment Report of the Intergovernmental Panel on Climate Change* (ed. S. Solomon, D. Quin, M. Manning, Z. Chen, M. Marquis, K. B. Averyt, M. Tignor and H. L. Miller), pp. 747-846. Cambridge: Cambridge University Press.
Mehrbach, C., Culberson, C. H., Hawley, J. E. and Pytkowicz, R. M. (1973). Measurement of apparent dissociation constants of carbonic acid in seawater at atmospheric pressure. *Limnol. Oceanogr.* **18**, 897-907.
O'Donnell, M. J., Hammond, L. T. M. and Hofmann, G. E. (2009). Predicted impact of ocean acidification on a marine invertebrate: elevated CO_2 alters response to thermal stress in sea urchin larvae. *Mar. Biol.* **156,** 439-446.
O'Donnell, M. J., Todgham, A. E., Sewell, M. A., Hammond, L. M., Ruggiero, K., Fangue, N. A., Zippay, M. L. and Hofmann, G. E. (2010). Ocean acidification alters skeletogenesis and gene expression in larval sea urchins. *Mar. Ecol. Prog. Ser.* **398**, 157-171.
Okazaki, K. and Inoue, S. (1976). Crystal property of larval sea urchin-spicule. *Dev. Growth Differ.* **18**, 413-434.
Oliveri, P., Tu, Q. and Davidson, E. H. (2008). Global regulatory logic for specification of an embryonic cell lineage. *Proc. Natl. Acad. Sci. USA* **105**, 5955-5962.
Parker, L. M., Ross, P. M. and O'Connor, W. A. (2009). The effect of ocean acidification and temperature on the fertilization and embryonic development of the sydney rock oyster *Saccostrea glomerata* (gould 1850). *Glob. Change Biol.* **15**, 2123-2136.
Peled-Kamar, M., Hamilton, P. and Wilt, F. H. (2002). Spicule matrix protein LSM34 is essential for biomineralization of the sea urchin spicule. *Exp. Cell Res.* **272**, 56-61.
Revilla-i-Domingo, R., Oliveri, P. and Davidson, E. H. (2007). A missing link in the sea urchin embryo gene regulatory network: hesC and the double-negative specification of micromeres. *Proc. Natl. Acad. Sci. USA* **104**, 12383-12388.
Sharma, T. and Ettensohn, C. A. (2010). Activation of the skeletogenic gene regulatory network in the early sea urchin embryo. *Development* **137**, 1149-1157.
Smith, J. and Davidson, E. H. (2008). Gene regulatory network subcircuit controlling a dynamic spatial pattern of signaling in the sea urchin embryo. *Proc. Natl. Acad. Sci. USA* **105**, 20089-20094.
Sultan, S. E. (2007). Development in context: the timely emergence of eco-devo. *Trends Ecol. Evol. (Amst.)* **22**, 575-582.
Todgham, A. E. and Hofmann, G. E. (2009). Transcriptomic response of sea urchin larvae *Strongylocentrotus purpuratus* to CO_2-driven seawater acidification. *J. Exp. Biol.* **212**, 2579-2594.
Urry, L. A., Hamilton, P. C., Killian, C. E. and Wilt, F. H. (2000). Expression of spicule matrix proteins in the sea urchin embryo during normal and experimentally altered spiculogenesis. *Dev. Biol.* **225**, 201-213.
Wei, Z., Angerer, R. C. and Angerer, L. M. (2006). A database of mRNA expression patterns for the sea urchin embryo. *Dev. Biol.* **300**, 476-484.
Wikramanayake, A. H., Peterson, R., Chen, J., Huang, L., Bince, J. M., McClay, D. R. and Klein, W. H. (2004). Nuclear beta-catenin-dependent Wnt8 signaling in vegetal cells of the early sea urchin embryo regulates gastrulation and differentiation of endoderm and mesodermal cell lineages. *Genesis* **39**, 194-205.
Wilt, F. H. (2005). Developmental biology meets materials science: morphogenesis of biomineralized structures. *Dev. Biol.* **280**, 15-25.
Wilt, F. H., Killian, C. E., Hamilton, P. and Croker, L. (2008a). The dynamics of secretion during sea urchin embryonic skeleton formation. *Exp. Cell Res.* **314**, 1744-1752.
Wilt, F. H., Croker, L., Killian, C. E. and McDonald, K. (2008b). Role of lsm34/spsm50 proteins in endoskeletal spicule formation in sea urchin embryos. *Invertebr. Biol.* **127**, 452-459.
Wolpert, L. (1992). Gastrulation and the evolution of development. *Dev. Suppl.* **116**, 7-13.
Wu, S. Y. and McClay, D. R. (2007). The Snail repressor is required for PMC ingression in the sea urchin embryo. *Development* **134**, 1061-1070.